optica

Observation of subluminal twisted light in vacuum

Frédéric Bouchard,[1,2] Jérémie Harris,[1,2] Harjaspreet Mand,[1,2] Robert W. Boyd,[1,2,3] and Ebrahim Karimi[1,2,*]

[1]Department of Physics, University of Ottawa, 25 Templeton St., Ottawa, Ontario K1N 6N5, Canada
[2]The Max Planck Centre for Extreme and Quantum Photonics, University of Ottawa, Ottawa, Ontario K1N 6N5, Canada
[3]Institute of Optics, University of Rochester, Rochester, New York 14627, USA
*Corresponding author: ekarimi@uottawa.ca

Received 9 December 2015; revised 27 January 2016; accepted 2 February 2016 (Doc. ID 255400); published 23 March 2016

Einstein's theory of relativity establishes the speed of light in vacuum, c, as a fundamental constant. However, the speed of light pulses can be altered significantly in dispersive materials. While significant control can be exerted over the speed of light in such media, to our knowledge no experimental demonstration of altered light speeds has hitherto been achieved in vacuum for "twisted" optical beams. We show that "twisted" light pulses exhibit subluminal velocities in vacuum, being 0.1% slowed relative to c. This work does not challenge relativity theory but experimentally supports a body of theoretical work on the counterintuitive vacuum group velocities of twisted pulses. These results are particularly important given recent interest in applications of twisted light to quantum information, communication, and quantum key distribution.

OCIS codes: (260.0260) Physical optics; (080.4865) Optical vortices; (070.7345) Wave propagation.

http://dx.doi.org/10.1364/OPTICA.3.000351

Velocity, the rate at which an object changes its position over time, is well-defined for Newtonian particles, but cannot in general be unambiguously assigned to waves. For the specific and unphysical case of a monochromatic plane wave, however, a propagation rate, referred to as the phase velocity, can be attributed to the beam phase front. The phase velocity v_{ph} of a monochromatic plane wave in a medium with refractive index n is given by c/n. A more general expression for v_{ph} is required when considering the propagation of a light beam with phase front $\Phi(\mathbf{r})$, $v_{\mathrm{ph}} = \omega/|\nabla\Phi|$, where ω denotes the angular frequency of the beam and ∇ represents the gradient with respect to the spatial coordinate $\mathbf{r}$ [1]. A pulsed beam, which is spatiotemporally localized, is comprised of an infinite superposition of monochromatic waves, each of which propagates at a distinct phase velocity $v_{\mathrm{ph}}(\omega)$. It is the constructive and destructive interference among these frequency components that gives rise to the pulse shape and position. As a result, the pulse propagates at a speed different from that of the individual monochromatic waves of which it is composed. The speed at which the pulse envelope propagates is referred to as the group velocity v_g and is given by $v_g = |\partial_\omega \nabla\Phi|^{-1}$, where ∂_ω stands for differentiation with respect to ω [1]; see Supplement 1 for more details.

The refractive index of a nondispersive medium does not depend on the frequency of light being considered. Consequently, the phase and group velocities associated with a plane wave propagating along a nondispersive medium's z axis will take on the values $v_{\mathrm{ph}} = v_g = c/n$, since $\Phi = (\omega n/c)z$. In contrast to plane waves, the phase and group velocities of light pulses can differ by orders of magnitude in dispersive media such as cold atomic clouds [2], atomic vapors [3,4], and structurally engineered materials [5–7]. Under such exotic conditions, pulse group velocities can be rendered greater or smaller than c, or even negative [8]. Here we investigate the exotic group velocities exhibited by Laguerre–Gauss (LG) modes in vacuum. In particular, we observe and explain subluminal effects that arise due to the twisted nature of the optical phase front. We use an experimental setup that employs nonlinear intensity autocorrelation to measure relative time delays between Gaussian and twisted beams, and show these time delays to be significant, in some cases reaching several tens of femtoseconds. Our theoretical treatment predicts that further exotic effects, such as superluminal propagation in vacuum, might also manifest themselves as a consequence of the structured light beams.

Despite their mathematical simplicity, plane waves carry infinite energy and therefore are unphysical. More complex waves that can only be approximated even under ideal experimental conditions, such as Bessel beams and evanescent waves, have been studied for their exotic group velocities in vacuum [9,10]. A recent publication has also reported slow-light effects in vacuum [11] for both Gaussian and Bessel-like beams. The work demonstrated light delays as large as ~27 fs. The observed effect here and that of Giovannini *et al.* [11] are comparable in magnitude, although different in nature, as the latter results from a "tilting" of the wave vector. Giovannini *et al.* reported that the optical group delay increased with the square of the diameter of the beam, keeping all other parameters constant. Although their model has been validated through a wave-optics analysis, they interpreted their results in terms of a ray-optics picture. In their ray-optics model, the slow-light effect occurs because a ray traveling from the edge of the beam to the focus traverses a larger distance than an axial ray. This model predicts that the group delay scales as the square

of the beam diameter. In the present work, we report that the group velocity decreases linearly with the OAM value ℓ of the beam. Because the diameter of an LG beam scales as the square root of the ℓ value, the scaling law that we observe is consistent with that reported by Giovannini *et al.* We have interpreted this dependence (see Supplement 1) as arising as a consequence of the twisted nature of the optical wavefront.

Physically realizable beams, which carry finite energy, possess spatial phase and intensity structures differing from those of plane waves. LG modes are among the most commonly encountered examples of such beams, and are solutions to the paraxial wave equation. It may therefore be more transparent to frame the initial theoretical development in the language of pure LG modes, which serve as a more natural basis in which to consider slow-light effects in vacuum arising from a twisting of optical wavefronts. Notwithstanding the aesthetic and pedagogical appeal of a pure-LG-mode theory, our experiment is carried out using vortex beams, such as hypergeometric Gaussian (HyGG) ones, as these are more readily generated experimentally for reasons that will be made clear later [12]. LG modes are an orthonormal and complete set, in terms of which any arbitrary paraxial mode can be expanded [13], including HyGG modes. They are characterized by azimuthal and radial mode indices, ℓ and p, respectively. These modes are eigenstates of orbital angular momentum (OAM), and in vacuum carry OAM values of $\ell\hbar$ per photon along their propagation direction [14,15]. LG modal transverse intensity profiles feature intensity maxima at $r_{\max} = w(z)\sqrt{|\ell|/2}$, where $w(z)$ is the beam radius upon propagation [16]. The LG mode phase fronts have helical structures, and in vacuum are given by

$$\Phi^{\mathrm{LG}}(\mathbf{r}, \omega) = \frac{\omega}{c} z + \frac{\omega r^2}{2cR} + \ell\varphi - (2p + |\ell| + 1)\zeta, \qquad (1)$$

where $R := R(z, \omega)$ is the radius of curvature of the beam phase front, $\zeta := \zeta(z, \omega)$ is the Gouy phase [17], defined in Supplement 1, and r, φ, z are the standard cylindrical coordinates. The dependence exhibited by Φ^{LG} on its spatial coordinates $\mathbf{r}$, angular frequency ω, and the indices ℓ and p suggests that the phase velocity of these LG modes also depends on these values. Indeed, when explicitly calculated, the phase velocity is found to depend on r, ω, ℓ, and p, i.e., $v_{\mathrm{ph}}(r, z; \omega; p, \ell)$. This concept is illustrated in Fig. S1 of Supplement 1, which shows the spatial dependence of the phase fronts associated with Gaussian and spherical waves. This phase velocity leads to the conclusion that v_g is a function of r, z, ω, p, and ℓ, i.e., $v_g(r, z; \omega; p, \ell)$.

The group velocity is calculated by means of a procedure described in Supplement 1, where we also show that the slow-light effect arises largely from the structure of the wavefront radius of curvature, as distinct from the Gouy phase effect already discussed in the theoretical literature [18–20]. Indeed, the Gouy phase effect is an order of magnitude smaller than that observed in our experiment. Notably, the slow-light effects investigated here are observed to arise due to the twisting of the optical phase front itself, which causes the beam's intensity maximum to follow a hyperbolic trajectory.

The group velocities associated with LG modes having different p and ℓ indices are shown as functions of distance in Fig. 1. Figure 1(a) demonstrates that beams with $\ell = 0$ propagate at subluminal and superluminal speeds depending on propagation distance for all values of p. Specifically, for propagation distances bounded by $|z| \le z_R$, these modes exhibit superluminal speeds,

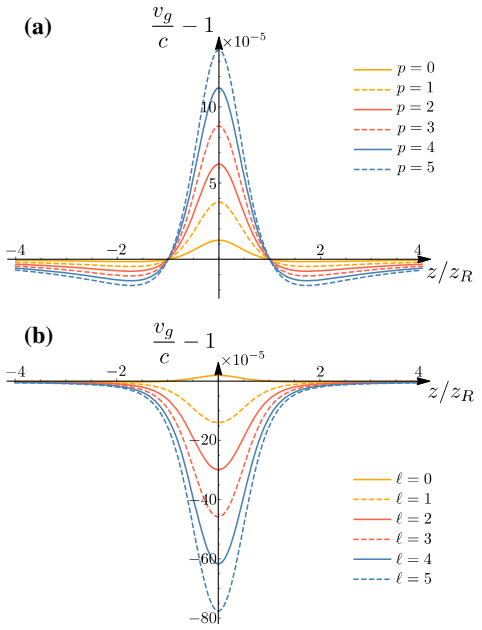

Fig. 1. Group velocities of focused Laguerre–Gauss modes as a function of propagation distance. (a) Group velocities as a function of propagation distance for LG modes with $\ell = 0$ and various values of p. These velocities pertain to the on-axis case, $r = 0$. Three different propagation regions can be identified: a first subluminal zone $z < -z_R$, a superluminal zone $|z| < z_R$, and a second subluminal zone $z > z_R$, where $z_R = \omega w_0^2/(2c)$ is the Rayleigh range, at which all modes travel at speed c. (b) Propagation dependence of group velocities for LG beams characterized by $p = 0$ and different values of ℓ. These group velocities are calculated not along the beam axis but at the radial position corresponding to the beam intensity maximum $r_{\max} = w(z)\sqrt{|\ell|/2}$. $r_{\max}$ defines the circle through which will pass all rays associated with a given LG mode in the ray tracing picture. With the exception of the $\ell = 0$ case, all modes are found to exhibit subluminal behavior throughout propagation. These results are obtained from simulations of light at a wavelength of 795 nm with a beam waist of 2.5 mm, focused by a thin lens of focal length 400 mm.

which at the waist increase linearly by $\delta v_g^{(p)} = 2.5 \times 10^{-5}$ cp for the fairly typical case of light at 795 nm with a beam waist of 100 μm. At the positions $z = \pm z_R$, where $z_R = \omega\, w_0^2/(2c)$ is the Rayleigh range, all modes propagate at c. Beyond z_R, subluminality can be observed. Despite their fast-light behavior at the waist, beams with $p \neq 0$ still lag behind the Gaussian mode as a result of their having experienced subluminal velocities prior to z_R.

The competing slow- and fast-light effects characterizing the propagation of $p \neq 0$ modes cancel to a significant extent for propagation distances beyond z_R, rendering p-index-induced pulse delays extremely difficult to measure. By contrast, for a fixed $p = 0$, LG modes are found to exhibit slow-light behavior for all propagation distances and all values of ℓ, as shown in Fig. 1(b). In this case, light speed reduction at the waist increases linearly with ℓ by $\delta v_g^{(\ell)} = -1.6 \times 10^{-4}\, c\ell$ for light at 795 nm with a beam waist of 100 μm. Although this effect is small, the time delay experienced by $\ell \neq 0$ pulses increases monotonically with propagation distance, reaching measurable values far from the waist. Nonetheless, the expected time delays for $\ell \neq 0$ relative to $\ell = 0$ Gaussian pulses are on the order of a few femtoseconds for the wavelength of light and beam waist considered, since the portions

of an $\ell \neq 0$ beam that are maximally intense experience more pronounced phase front curvature effects. A ray tracing picture, however, may be relied on in order to explain why beams carrying different OAM exhibit subluminal behaviors. In this picture, optical beams with higher values of OAM possess higher transverse wave vectors, so that the longitudinal components of their wave vectors are reduced. Therefore, their phase velocities are decreased as a consequence of increasing their OAM values. However, this geometrical optics picture is not fully accurate, since it is incapable of explaining superluminal effects of the sort observed in Fig. 1(a). Therefore, the need for a highly accurate arrival time measurement strategy is clearly indicated [11,21].

A schematic of our experimental setup is shown in Fig. 2. We measured the relative time delay between a Gaussian reference pulse and an $\mathrm{HyGG}_\ell = \sum_p c_p \mathrm{LG}_{p,\ell}$ pulse by implementing a technique analogous to noncollinear intensity autocorrelation (see Supplement 1 for more details) is more accurate. We spatially overlap these noncollinear pulsed beams inside a beta-barium borate (BBO) nonlinear crystal. A time delay is introduced between the two pulses using an optical delay stage. When this delay is minimized, the pulses are spatially and temporally overlapped within the crystal, leading to maximization of the noncollinear second-harmonic generation output pulse intensity. In this way, time delays experienced by the test beam can be detected by measuring the delay stage movement required to restore maximal pulse overlap. Using this technique, changes in relative arrival times of the Gaussian and twisted pulses induced by increases in the HyGG mode ℓ index can be measured within femtoseconds.

Figure 3(a) shows normalized power measured as a function of the delay stage position using the autocorrelation technique described (see Supplement 1), for HyGG modes with various values of ℓ. As can be seen, measurable shifts occurred between all HyGG modes presented in the figure. These peak shifts arise from differences in the pulse arrival time induced by the subluminal

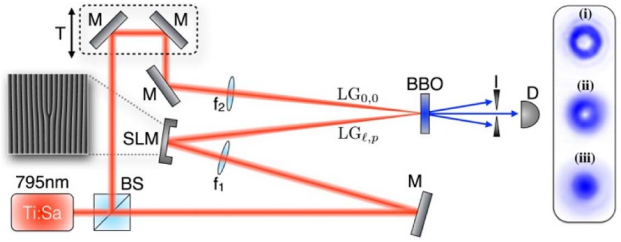

Fig. 2. Experimental setup for measuring subluminal speeds of twisted pulsed beams in vacuum. The test HyGG_ℓ beam is generated using a spatial light modulator (SLM) onto which is displayed the hologram shown in the figure. Reference $\mathrm{LG}_{0,0}$ and test HyGG_ℓ beams are focused into a type-I beta-barium borate (BBO) crystal. Second-harmonic generation (SHG) output transverse intensity profiles of the test, cross, and reference beams are shown in parts (i)–(iii) of the rightmost inset. When the delay between the test and reference arms is on the order of the pulse duration, one photon from each can be upconverted to produce an SHG photon. By conservation of linear momentum, this photon will exit the BBO crystal at the bisector between the SHG beams produced by the test and reference beams alone. Conservation of OAM further requires that the SHG outputs (i)–(iii) carry OAM values of 2ℓ, ℓ, and 0 [22,23]. The inset shows beam profiles obtained experimentally for the case $\ell = 1$. Note that the hologram shown here generates a pure ℓ mode with an infinite superposition of p modes, where most of the power resides in the fundamental $p = 0$ mode. Legend: BS-beam splitter, T-delay line (trombone), M-mirror, f-lens, I-iris, and D-detector.

speeds experienced by different HyGG beams during propagation. In particular, the shift in peak position between the $\mathrm{LG}_{0,0}$ and HyGG_6 modes is approximately 7 μm, corresponding to a time delay of 23 fs, from which can be inferred a maximum fractional group velocity drop of 0.1% relative to c. This fractional velocity drop is determined from the theoretical curves plotted in Fig. 1.

The velocity drop recorded here is that corresponding to the $z = 0$ propagation position, and it therefore represents the slowest pulse propagation speed reached during the experiment. Time delays experienced by various HyGG_ℓ modes relative to the $\mathrm{LG}_{0,0}$ reference mode are shown in Fig. 3(b). These results reveal the expected linear dependence of pulse arrival time on ℓ for a specific propagation distance (see Supplement 1). This dependence may be understood with reference to Eq. (1), which indicates that phase is a function of the index ℓ and the radial curvature $R(z, \omega)$. While the ℓ index is clearly shown to play an important role in determining the group velocity of an LG mode, the effect of the p index is far less pronounced, for reasons discussed earlier. Thus, HyGG and LG beams will experience similar time delays, up to some correction factor. In the far-field, the group velocity of any LG mode asymptotically approaches c; see Fig. 1. Therefore, the time delay between $\mathrm{LG}_{p,\ell}$ and $\mathrm{LG}_{0,0}$ reaches a constant value far from the focus.

A number of conclusions can be drawn from the investigation presented here. First, the group velocities of twisted LG beams (HyGG beams) have been shown to differ measurably from those of Gaussian pulses, even in free space. This surprising phenomenon can be interpreted as arising from diffraction effects in

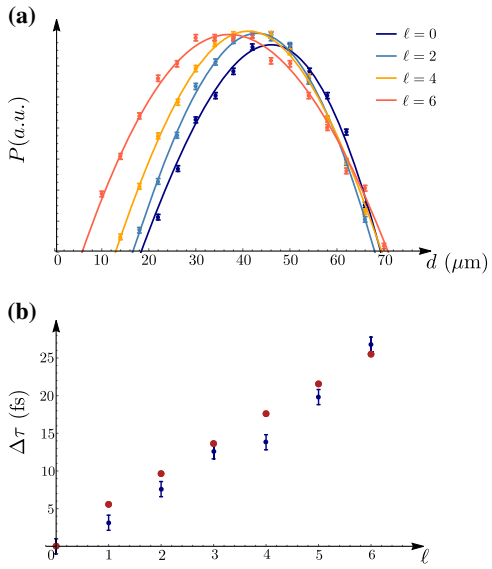

Fig. 3. Subluminal light propagation of HyGG modes in free space. (a) Normalized power obtained from the autocorrelation technique described in the text as a function of delay stage position, d, for HyGG beams with $\ell = 0, 2, 4, 6$. Raw data are presented along with the fits used to estimate pulse peak positions. Power was measured at each stage position over a period of sufficient length to suppress Poissonian noise. The widths of the autocorrelation traces were found to fall in the range of 201 ± 6 μm, but in the interest of clarity, only the peaks of the autocorrelation traces are shown. (b) Arrival times of HyGG_ℓ pulses relative to an $\mathrm{LG}_{0,0}$ reference pulse extracted from peak positions determined directly from experimental data. A linear relationship between arrival time and ℓ is observed, and the experimental data (blue dots) are plotted along with theoretical data (red dots) obtained from the group velocity expression derived in Supplement 1.

vacuum, as it results in wavelength-dependent phase and group velocities. This is different from the standard approach to calculating group velocities for a pulse in a medium considering the dispersion relation. Further, exotic phase and group velocity effects inevitably arise for any physically realizable beam, for these must necessarily possess nontrivial spatial amplitude and phase structures, which result in other-than-luminal propagation speeds. For the particular case of twisted light, spatial structure can lead to slow-light effects whose magnitudes depend directly on various beam parameters, including the modal ℓ and p indices.

These findings carry great practical significance, particularly for classical and quantum communication and quantum information with twisted light [24–26]. Single photon sources have a limited pulse width, which depends on the pump pulse duration. Although it is possible to implement some of the quantum protocols, such as the decoy state quantum key distribution (QKD), with an attenuated coherent state, most of the quantum information schemes require photons to have a certain temporal coherence. This temporal coherence length is on the order of several tens of micrometers (femtosecond duration), which is exactly the temporal length of the laser pulse that we have studied. Therefore, our results, both theoretical model and experimental results, are valid for the case of single photons as well. In light of significant recent interest in implementing QKD and quantum computations with structure photons, one must take the presented subluminal effect for twisted photons into account.

Unless differences induced in LG mode pulse arrival times are compensated for, the subluminial and superluminal effects reported here could result in the out-of-sequence detection of pulses, or the failure of quantum logic gates. A photon in an OAM qubit state $|\psi_{\alpha,\beta}\rangle = (\alpha|0\rangle + \beta|\ell\rangle)$, where $|0\rangle$ and $|\ell\rangle$, respectively, represent $LG_{0,0}$ and $LG_{0,\ell}$ modes, generated by a sender (Alice) at time $t = 0$ will travel at a group velocity that depends on the values of α and β. As a result, the photon's arrival time at the receiver (Bob) will be given by $t_{\alpha,\beta} = \int_{z=\text{source}}^{z=\text{reciever}} dz/v_g^{\alpha,\beta}(z)$. As this treatment shows, the message will reach Bob at a time that will depend on α and β. More generally, photons associated with an arbitrary mode $|\psi_{\{c_\ell\}}\rangle = \sum_{\ell=0}^{+\infty} c_\ell|\ell\rangle$ will exhibit arrival times $t_{\{c_\ell\}}$, which will depend on the set $\{c_\ell\}$ of amplitudes associated with each LG component comprising the beam of interest.

Photon OAM has been shown to represent a valid state label that can be used to distinguish one photon from another. From a quantum information standpoint, therefore, one could imagine how a Hong–Ou–Mandel (HOM)-type experiment could exhibit great sensitivity to the slow-light effects explored here. In particular, a HOM experiment carried out, for example, with one photon in an $LG_{0,0}$ mode and the other in a coherent superposition of $LG_{0,0}$ and $LG_{0,1}$ modes would already be expected to register only a limited dip, due to the partial distinguishability of the two photons on the basis of their OAM. However, our work has shown that a second effect will also be at play: in addition to being damped due to the partial distinguishability of the incident photons, one would also expect the HOM dip obtained in such an experiment to be *skewed* as a direct consequence of the different arrival times of the two photons. Given the critical importance of the HOM effect in quantum information protocols, this second effect may have a wide range of practical consequences.

Notably, our results should not be misattributed to lens thickness effects [27], which have been avoided by removing any lenses in the path of the LG beam following its generation. We have shown that time delays on the order of several femtoseconds can arise between LG modes due to the group velocity effects we have explored, depending on the geometries of the sender and receiver optics. As a result, any communication scheme [28,29] or computation protocol [30] relying on twisted light must account for the slow and fast light effects that we have demonstrated.

Funding. Canada Research Chairs; Canada Excellence Research Chairs (CERC); Government of Canada; Natural Sciences and Engineering Research Council of Canada (NSERC).

Acknowledgment. We thank Peter Banzer and Miles J. Padgett for fruitful discussions.

See Supplement 1 for supporting content.

REFERENCES

1. M. Born and E. Wolf, *Principles of Optics: Electromagnetic Theory of Propagation, Interference and Diffraction of Light* (Cambridge University, 1999), Chap. 1.
2. L. V. Hau, S. E. Harris, Z. Dutton, and C. H. Behroozi, Nature **397**, 594 (1999).
3. A. Dogariu, A. Kuzmich, and L. Wang, Phys. Rev. A **63**, 053806 (2001).
4. M. S. Bigelow, N. N. Lepeshkin, and R. W. Boyd, Science **301**, 200 (2003).
5. M. Notomi, K. Yamada, A. Shinya, J. Takahashi, C. Takahashi, and I. Yokohama, Phys. Rev. Lett. **87**, 253902 (2001).
6. N.-H. Liu, S.-Y. Zhu, H. Chen, and X. Wu, Phys. Rev. E **65**, 046607 (2002).
7. J. Sharping, Y. Okawachi, and A. Gaeta, Opt. Express **13**, 6092 (2005).
8. G. M. Gehring, A. Schweinsberg, C. Barsi, N. Kostinski, and R. W. Boyd, Science **312**, 895 (2006).
9. N. V. Budko, Phys. Rev. Lett. **102**, 020401 (2009).
10. K. B. Kuntz, B. Braverman, S. H. Youn, M. Lobino, E. M. Pessina, and A. I. Lvovsky, Phys. Rev. A **79**, 043802 (2009).
11. D. Giovannini, J. Romero, V. Potoček, G. Ferenczi, F. Speirits, S. M. Barnett, D. Faccio, and M. J. Padgett, Science **347**, 857 (2015).
12. E. Karimi, G. Zito, B. Piccirillo, L. Marrucci, and E. Santamato, Opt. Lett. **32**, 3053 (2007).
13. A. E. Siegman, *Lasers* (University Science, 1986).
14. L. Allen, M. W. Beijersbergen, R. Spreeuw, and J. Woerdman, Phys. Rev. A **45**, 8185 (1992).
15. M. Padgett, J. Courtial, and L. Allen, Phys. Today **57**(5), 35 (2004).
16. M. Berry and K. McDonald, J. Opt. A **10**, 035005 (2008).
17. T. Visser and E. Wolf, Opt. Commun. **283**, 3371 (2010).
18. Z. Horváth, J. Vinkó, Z. Bor, and D. Von der Linde, Appl. Phys. B **63**, 481 (1996).
19. M. A. Porras, I. Gonzalo, and A. Mondello, Phys. Rev. E **67**, 066604 (2003).
20. R. J. Mahon and J. A. Murphy, J. Opt. Soc. Am. A **30**, 215 (2013).
21. R. Trebino, K. W. DeLong, D. N. Fittinghoff, J. N. Sweetser, M. A. Krumbügel, B. A. Richman, and D. J. Kane, Rev. Sci. Instrum. **68**, 3277 (1997).
22. T. Roger, J. J. Heitz, E. M. Wright, and D. Faccio, Sci. Rep. **3**, 3491 (2013).
23. J. Courtial, K. Dholakia, L. Allen, and M. Padgett, Phys. Rev. A **56**, 4193 (1997).
24. G. Gibson, J. Courtial, M. J. Padgett, M. Vasnetsov, V. Pas'ko, S. M. Barnett, and S. Franke-Arnold, Opt. Express **12**, 5448 (2004).
25. G. Molina-Terriza, J. P. Torres, and L. Torner, Nat. Phys. **3**, 305 (2007).
26. E. Nagali, L. Sansoni, F. Sciarrino, F. De Martini, L. Marrucci, B. Piccirillo, E. Karimi, and E. Santamato, Nat. Photonics **3**, 720 (2009).
27. E. Karimi, C. Altucci, V. Tosa, R. Velotta, and L. Marrucci, Opt. Express **21**, 24991 (2013).
28. J. Wang, J. Yang, I. M. Fazal, N. Ahmed, Y. Yan, H. Huang, Y. Ren, Y. Yue, S. Dolinar, M. Tur, and A. E. Willner, Nat. Photonics **6**, 488 (2012).
29. M. Krenn, R. Fickler, M. Fink, J. Handsteiner, M. Malik, T. Scheidl, R. Ursin, and A. Zeilinger, New J. Phys. **16**, 113028 (2014).
30. F. Cardano, F. Massa, H. Qassim, E. Karimi, S. Slussarenko, D. Paparo, C. de Lisio, F. Sciarrino, E. Santamato, R. W. Boyd, and L. Marrucci, Sci. Adv. **1**, e1500087 (2015).